Solute Dispersion in Casson Blood Flow through an Artery with the Effect of Electric Field

Nur Husna Amierah Mohd Zaperi[1], Nurul Aini Jaafar[1,*]

[1] Department of Mathematical Sciences, Faculty of Science, Universiti Teknologi Malaysia, 81310 Johor Bahru, Johor, Malaysia
* Correspondence: nurulaini.jaafar@utm.my
https://doi.org/10.37934/jrnn.9.1.1334

ABSTRACT

A condition of the heart or blood vessels is referred to as cardiovascular disease (CVD). When it comes to cancer, people with CVD are more likely to get it than people without it. The correlation between atherosclerosis and particular cancer subtypes, which remains even after adjusting for traditional risk factors, could contribute to this link. The motivation for this work is to analyse the steady flow of dispersion of solute in blood flow through an artery with the effect of an electric field. Blood is considered a Casson fluid model. The velocity of the Casson fluid model is determined by solving momentum and constitutive equations. The concentration of solute, dispersion function and mean concentration are obtained by using the Generalized Dispersion Model (GDM). The results are validated with the previous solution without the effects of electric field and stenosis. The results showed good conformity between the two solutions. An increase in electric field increases the velocity, steady dispersion function and mean concentration while reducing the unsteady dispersion function and dispersion function. It is observed that the solute dispersion in blood flow affects the electric field. Casson fluid is an appropriate fluid to investigate the blood velocity and transportation of the drug in blood flow to the targeted stenosed region through a very narrow artery for the treatment of arterial diseases.

1. Introduction

According to Shah *et al.,* [1], analysis of the fluid flow's solute dispersion procedure with relation to the wide range of applications in the medical sciences is the research field that holds the most interest. In a recent development, Chauhan and Tiwari [2] stated that substances like nutrients, medications and metabolic components are transported in the circulatory system as a result of the dispersion mechanism in physiological conditions. In the circulatory system, nutrition and waste are

transported through a complex combination of blood cells, lipoproteins, and ions. *Functions of blood: transport around the body* [3] stated that nutrients digested are taken up by the bloodstream through the intestine's tiny capillaries.

The investigation of flow via a pipe has always piqued the interest of mathematicians, primarily because of its direct relevance to the understanding of blood flow via arteries [4]. The mathematical modelling of the circulatory system elucidates the impact of multiple parameters on arterial blood circulation and the dispersion of solutes resulting from drug administration via the circulatory system into the tissues. Developing an accurate model for an artery is a challenging task due to the intricate network of arteries in the human body and their unique characteristics. The presence of an imbalanced lifestyle has the potential to exert adverse effects on the health of the coronary arteries, hence contributing to the development of cardiovascular disease (CVD). Examples of such lifestyle factors include smoking, eating fast food, being sedentary, having high cholesterol, and having diabetes. Heart disease encompasses a wide range of conditions, most of which are brought on by atherosclerosis. Atherosclerosis is a progressive plaque disorder that can begin in childhood and worsen with time. Atherosclerosis gradually takes over as a result of the plaque that is created by blood cells, fat, cholesterol, and other substances. When the plaque builds up, the arteries get narrower. Consequently, less oxygen-rich blood is supplied to the body's vital organs [5]. Therefore, research on stenosed arteries can potentially improve the medical treatment of stenosis and contribute to fluid mechanic studies regarding the flow in the stenosed arteries.

As a result of CVD, the overall prevalence of cancer may grow. Hypertension, obesity, smoking, diabetes, and an unhealthy diet and lifestyle all contribute to cancer development. Cancer is an uncontrolled cell growth. Cells turn cancerous if certain mutations take place in the several genes that influence cell growth. Cancer cells remain in the bodily tissue from which they originated. Cancerous tissue cells grow and multiply in order to produce additional cells, eventually forming a tumour. Hence, investigating the solute dispersion in blood circulation holds significance as it contributes to the accumulation of comprehensive understanding regarding the molecular mechanisms behind the initiation, progression, and metastasis of cancer inside the human body. The aforementioned discoveries have resulted in the development of treatments that are more efficient and focused, as well as tactics for medication administration and prevention that have proven to be beneficial.

Several novel medication delivery methods are being utilized in cancer treatment. Chemotherapy is one of the most often used cancer therapies. It employs specific medications to either kill cancer cells or prevent cancer cells from developing and spreading to other regions of the body [6]. As a result, it is preferable to design chemotherapeutics that may either passively or actively target malignant cells, lowering side effects while boosting therapeutic efficacy. The electric field in the blood may influence cancer cell alterations. The data generated by this effect will assist the doctor in determining the dose rate necessary for the cancer patient's body.

Yield stress is a useful Casson fluid for emulating blood circulation in tiny vessels. A Casson fluid is, as is well known, a shear-thinning fluid with an infinite shear rate, infinite yield stress, and zero viscosity. Blair [7] showed that the basic blood shear dynamics in tiny arteries may be described using Casson's fluid model. In the investigation of blood circulation properties, Casson [8] investigated the applicability of the Casson fluid model and determined that blood exhibits a nonzero yield stress at low shear rates. According to Merrill *et al.,* [9], circulatory system characteristics inside tubes with diameters varying from $130-1000\mu m$ can be precisely predicted by the Casson fluid. Therefore, Casson fluid can be considered an appropriate model for blood flow analysis.

Some CVDs are caused by arterial stenosis. The best CVD treatment depends on the patient [10]. Medication, surgery, and cardiac rehabilitation are options. Treatment aims to relieve symptoms,

reduce the risk of recurrence, and prevent hospital stays, heart attacks, strokes, and heart failure. Cardiovascular disease risk factors include obesity, diabetes, high cholesterol, and hypertension [10]. Various factors affecting the stenosed artery should be evaluated to reduce complications. Many factors affect blood flow and solute dispersion, including stenosis size. Doctors can determine patient medicine dosage by considering stenosis height and length. The continuous flow of solute in blood flow must be analysed to observe the solute and blood to ensure a realistic representation of drug distribution through the stenosed artery and increase drug efficacy by giving patients precise drug dosages. Therefore, stenosed artery research is needed to understand blood flow and solute dispersion.

Cancer can result from CVD. One cancer treatment is chemotherapy. Cancer treatment can cause many side effects. Side effects of cancer treatment include harming healthy cells or removing organs after surgery [11]. Side effects vary by person, medicine, and therapy. Hair loss, vomiting, and neutropenia—a reduction in white blood cells, the body's main line of defence—are typical adverse results of cancer therapy [11]. However, electric field effects on solute dispersion in stenosed arterial blood flow should be considered. This prevents the electric fields from affecting blood flow and artery solute dispersion.

The investigation of Casson fluid flow properties in tubes was conducted by Roy *et al.*, [12]. Roy *et al.*, [12] utilized the Casson fluid model to study reactive species dispersion under oscillatory flow conditions. Pulsatile pressure gradients inspired this study, which used the Aris-Barton method to solve the mathematical equations. Debnath *et al.*, [13] used the Aris-Barton approach to obtain the mathematical equations for the transit of a solute via an annular conduit in a Casson fluid with a repeating pulsatile pressure gradient due to heterogeneous chemical processes. This research studies annulus cross-section solute concentration distribution. Debnath *et al.*, [14] studied the wall reaction that affects species transport in annular pulsatile Casson fluid flow. The dispersion coefficient and the technique of moments are used to analyse the transport process. Advection, dispersion, and exchange coefficients are used to study transport phenomena. Yield stress, wall responses, phase exchange rate kinetics, radius ratio, and irreversible absorption rate affect these coefficients. A porous channel that conforms to the Darcy-Forchheimer theory was studied by Ali *et al.*, [15] for heat transfer properties and mass characteristics of pulsating flow. The study examined Casson fluid hybrid nanofluid (HNF) behaviour to understand blood circulation in arteries with stenosis. The mathematical solutions are solved numerically using the finite-difference flow solver. This solver uses a vorticity stream function. Singh and Murthy [16] studied unstable solute dispersion in circular tube pulsatile non-Newtonian flow. The researchers employed Aris's moments technique to investigate higher-order moments. The Luo and Kuang (1992) constitutive relation, or K-L Model, describes non-Newtonian fluids. The analysis immediately produces Casson, Bingham, and Newtonian model results.

Dandu *et al.*, [44] investigated the unsteady magnetohydrodynamic with the effect of radiation absorption and diffusion thermodynamics using Casson fluid that inclined the moving plate in thermal radiation, heat absorption and homogenous chemical reactions and solved it using perturbation technique. Yahaya *et al.*, [45] analysed stagnation flow for two-dimensional magnetohydrodynamic (MHD) of incompressible Casson fluid with the effect of homogeneous-heterogeneous reactions, suction and slip effects, which was solved by using a partial differential equation. Omar *et al.*, [46] studied the unsteady Casson fluid model in a porous medium in the presence of thermal and chemical radiation by applying the partial differential equation. Azmi *et al.*, [47] studied the Casson fluid model in human blood flow in an artery by considering slip velocity at the boundary, which was solved by using the finite Hankel transform and the Laplace transform. Arifin *et al.*, [48] investigated the two-phase flow in real-life applications using Casson fluid, single-

wall carbon nanotubes (SWCNTs), and dust particles with the effects of the aligned magnetic field effect and Newtonian heating (NH). The Runge-Kutta-Kuttaerg (RKF45) method has been used to solve the mathematical equations. Mohamed *et al.,* [49] analysed boundary layer flow and heat transfer on slip effects on a horizontal plate using Casson ferrofluid and solved the problem using the Runge-Kutta-Fehlberg (RKF45) method.

In observing the blood circulation in an artery with the influence of temperature, it is preferable to add more effect to the blood flow to the artery under investigation to provide a more accurate depiction of the actual circumstances. Thus, taking into account the effect of an electric field on blood flow helps to better understand the behaviour of blood flow under the influence of temperature. Trivedi *et al.,* [17] stated that endothelial cells are exposed to the electro kinetic vascular streaming potential (EVSP), a pervasive but unstudied electrical force induced by blood circulation. By monitoring the production of nitric oxide and membrane potential under ELF conditions, this study evaluated the idea that the EVSP's extremely low-frequency (ELF) electric fields dramatically modify endothelial cell characteristics. Shit *et al.,* [18] used blood flow as micropolar fluid in a stenosed artery that is overlapped and tapering under an electric potential. Jin *et al.,* [19] examined autonomic nervous system responses to electrical stimulation. Interferential current (IFC) frequency and amplitude alter blood flow velocity and vessel size. Analysis by Tripathi *et al.,* [20] stated that electro kinetic peristaltic multi-layered transport is being studied in a micro-channel with an axial electrical field. The equations for mass and momentum preservation in a two-dimensional system with electro kinetic body forces are first converted, transitioning from the wave frame to the lab frame. The concepts of electric field in connection to electrical potential are made clear by the Poisson-Boltzmann equation, the ionic Nernst-Planck equation, and the Debye length approximation.

The micropolar fluid model was extensively studied by Tripathi *et al.,* [21] to determine the ways that microrotation affects blood flow dynamics. This work investigates the effects of electromagnetic fields, heat radiation, nanoparticle form, and electric double layer thickness on flow dynamics. Cylinders, bricks, and platelets are being studied as nanoparticle morphologies. Approximations of vast spatial scale, a small Reynolds number, and Debye-Hückel theory linearization solve the governing equations. Ramasamy and Murugan [22] used a low Reynolds number and zeta potential to solve the solute convection and dispersion coefficients for the axial movement of solute change in a circular tube with an outwardly provided electric field and the pulsatile flow of Carreau fluid. Murugan *et al.,* [23] used a generalized dispersion model to solve the dispersion in pulsatile electro-magneto-hydrodynamic flow in a tube filled with a porous medium using Casson fluid. Ponalagusamy and Murugan [24] examined the dispersion solute in pulsatile flow by considering the mechanism in a circular conduit using Carreau fluid, which was solved using GDM and the finite Hankel transform.

There exist numerous methodologies that are appropriate for investigating the dispersion of solutes, including the Taylor-Aris approach, the Aris-Barton method, and the GDM. In the study conducted by Taylor [25], the research focused on the phenomenon of solute dispersion inside a solvent in a linear pipe under conditions of steady flow. The solute exhibits diffusion because of the interaction between molecule diffusion and velocity variance throughout its cross-sectional area, resulting in the solute diffusing with molecular diffusivity, $\bar{D}_{eff} = \bar{a}^2 \bar{u}_m^2 / 48 \bar{D}_m$ where $\bar{a}$ is pipe radius, $\bar{u}_m$ is mean velocity and $\bar{D}_m$ is molecular diffusivity. The solute dispersion theory of Taylor showed by Aris [26] is only valid when $\bar{D}_{eff} > \bar{D}_m$. Then, Aris [26] introduced the Taylor-Aris dispersion method, which describes the impact of axial molecule diffusion. The latter theory was only viable for a limited time. The work of Taylor-Aris has been simplified by Gill [27] by the establishment of a

distribution for the local concentration, which is derived from a series expansion based on the mean concentration and is applicable for all time periods. Then, Gill and Sankarasubramanian [28] developed the first GDM to analyze the solute dispersion process. Gill and Sankarasubramanian [29] explored scattering in the presence of a wall response using exchange, convection, and scattering coefficients. Dash *et al.,* [30] used GDM to analyze unstable solute dispersion in Casson fluid flow. Rana and Murthy [31] studied solute dispersion in a small vessel under unsteady flow conditions. Two-phase Casson fluid models, power laws, and GDM were used to analyze the dispersion process with or without vessel wall solute absorption. Rana and Murthy [32] examined the process by which yield stress affects solute mobility in an unstable two-phase Casson fluid.

GDM was utilized to study solute dispersion in non-Newtonian flow in an inclined channel with porous beds by Ratchagar and Vijayakumar [33]. This model investigates the impact of magnetic fields and chemicals on the internal and exterior dispersion of solutes in blood flow. Guo *et al.,* [34] used high-order GDM terms to study solute transport in turbulent open channel flow. The vertical mean and spatial distribution of concentration must be described to analyze turbulent flow in channels that are opened. The direct solution of second-to-fourth-order dispersion models considers high-order variables. Jaafar *et al.,* [35] utilized the Herschel Bulkley (H-B) fluid model to study the way chemical reactions and variable stenosis heights destabilize solute dispersion in a limited artery with a cosine-curved stenosis. Solute dispersion functions are calculated by solving the convective-diffusion equation with the GDM. Chauhan and Tiwari [2] used two non-Newtonian fluids to study solute dispersion through absorbent micro-vessels under Herschel-Bulkley and Jeffrey viscosity assumptions. The issue was resolved using GDM. GDM is suitable for this study. GDM is reliable for solute dispersion and mean concentration in various arteries, according to this literature. Thus, GDM is appropriate.

To the best of the authors' knowledge, despite a physiologically plausible scenario in which drugs are transported or solutes are injected into the human circulatory system to treat medical conditions, the solute's dispersion during blood circulation through a vessel with the effect of an electric field using the Casson fluid model has not received enough attention. Thus, the goal of this research is to use the Casson fluid model to examine the steady flow behavior of blood in an artery under the influence of an electric field. The present investigation aims to develop a mathematical model of the Casson fluid model via blood circulation, resolve the momentum and continuity equation of blood flow, solve the unsteady convective-diffusion equation to obtain solute concentration, dispersion function, and mean concentration through GDM, and examine the effect of an electric field on solute dispersion in blood flow. The momentum equation is solved analytically to determine the blood flow velocity. Mathematical equations of the momentum equation have also been generated using the Navier-Stokes equation and the Maxwell equation. Additionally, GDM was obtained analytically by deriving mathematical formulations of convective diffusion coefficients, and GDM was then used to determine the dispersion function and mean concentration. Due to their very broad expressions, the momentum equation and convective diffusion coefficient are not discussed in detail.

2. Materials and Methods

2.1 Mathematical Formulation

Casson fluid was utilized to imitate blood. Micro-channels are modelled as a flow of fluids because blood can be isolated plasma fluid and cells can be injected with core fluid when it flows through microchannels [36]. The blood flow is measured using the system of polar cylindrical

coordinates $\left(\bar{r},\bar{\psi},\bar{z}\right)$, where the radial and axial coordinates designated by $\bar{r}$ and $\bar{z}$ respectively and the azimuthal angle denoted by $\bar{\psi}$. Figure 1 shows the geometry of pipe flow for Casson fluid model where $\bar{L}$ is the length of conduit, R_0 is the artery's radius, $\bar{\psi}$ is the azimuthal angle, $\bar{r}_p$ is the radius of the plug region in circular pipe, $\bar{\delta}$ is stenosis height, $\bar{u}$ is the velocity of fluid flow, $\bar{E}_z$ is electric field and $\bar{z}$ is the axial coordinate for circular pipe.
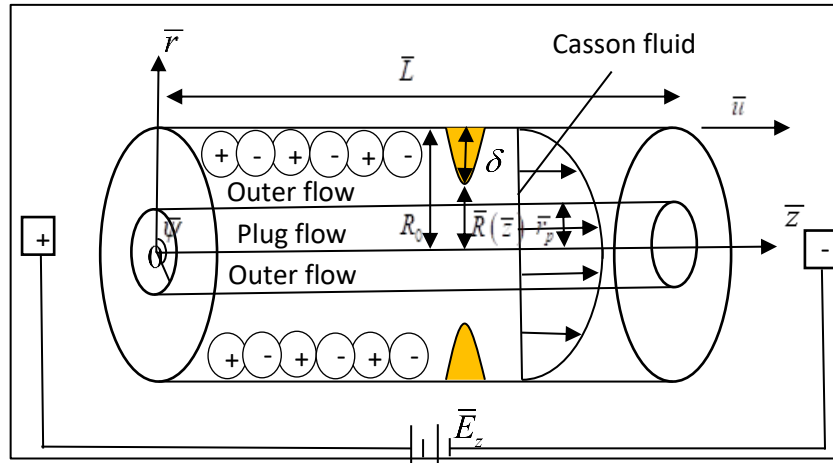
Fig. 1. The geometry of pipe flow for Casson fluid model with the effect of electric field

2.2 Governing Equations

The momentum equation which governs the flow is given as follows [37]

$$\mu\left[\frac{1}{\bar{r}}\frac{d}{d\bar{r}}\left(\bar{r}\bar{\tau}\right)\right]-\frac{d\bar{p}}{d\bar{z}}+\sigma\rho_e\bar{E}_z=0, \tag{1}$$

where the variables of μ, $\bar{\tau}$, $\bar{p}$, $\bar{\rho}_e$, σ and $\bar{E}_z$ are the viscosity of fluid, the shear stress, the fluid pressure, the fluid density in electric field, the conductivity of electricity and the electric field. The boundary condition for momentum equation is given as

$$\bar{\tau}=\text{finite at }\bar{r}=0. \tag{2}$$

The constitutive equation is defined as

$$-\frac{d\bar{u}}{d\bar{r}}=\begin{cases}\frac{1}{\mu}\left(\sqrt{\bar{\tau}}-\sqrt{\bar{\tau}_y}\right)^2 & \text{if }\bar{\tau}>\bar{\tau}_y,\\0 & \text{if }\bar{\tau}\leq\bar{\tau}_y,\end{cases} \tag{3}$$

where $\bar{u}$, $\bar{\tau}_y$, μ are the velocity of the fluid flow, the yield stress and the coefficient of viscosity for the Casson fluid model. The slip boundary condition for constitutive equation is given by Verma *et al.,* [38]

$$\bar{u} = \bar{u}_s \text{ at } \bar{r} = \bar{R}(\bar{z}), \tag{4}$$

where

$$\bar{R}(\bar{z}) = R_0 \left(1 - \frac{\bar{\delta}}{R_0} \exp\left(-\frac{\bar{k}^2 \bar{\varepsilon}^2 \bar{z}^2}{R_0^2} \right) \right), \tag{5}$$

where $\bar{R}(\bar{z})$ is the stenosed segment's radius, $\bar{\delta}$ is the stenosis height at the central point and $\bar{k}$ is the constant in parameters and radius, $\bar{\varepsilon} = R_0 / \bar{L}_0$. Consider the geometry of stenosis in Figure 1 in Eq. (5) as below

$$\frac{\bar{R}(\bar{z})}{R_0} = 1 - a e^{-bz^2}, \tag{6}$$

where $a = \bar{\delta} / R_0$ and $b = \bar{k}^2 \bar{\varepsilon}^2 / R_0^2$ are the variables in $\bar{R}(\bar{z})$. Non-dimensional for Eq. (6) as below

$$R(z) = 1 - a_1 e^{\left(-b_1 z^2 \right)}, \tag{7}$$

where $a_1 = \delta$ and $b_1 = b R_0^2$ are variables in $R(z)$.

The mean velocity is stated as below

$$\bar{u}_m = \frac{2}{\bar{R}^2(\bar{z})} \left[\int_0^{\bar{r}_p} \bar{u}(\bar{r}_p) \bar{r} d\bar{r} + \int_{\bar{r}_p}^{\bar{R}(\bar{z})} \bar{u}(\bar{r}) \bar{r} d\bar{r} \right]. \tag{8}$$

Then, two-dimensional unsteady convective-diffusion equation is expressed as follows:

$$\frac{\partial \bar{C}}{\partial \bar{t}} + u \frac{\partial \bar{C}}{\partial \bar{z}^*} = \bar{D}_m \left(\frac{1}{\bar{r}} \frac{\partial}{\partial \bar{r}} \left(\bar{r} \frac{\partial}{\partial \bar{r}} \right) + \frac{\partial^2}{\partial \bar{z}^{*2}} \right) \bar{C}. \tag{9}$$

Simplify Eq. (9), it yields

$$\frac{\partial \bar{C}}{\partial \bar{t}} + \bar{u} \frac{\partial \bar{C}}{\partial \bar{z}^*} = \bar{D}_m \left(\ell^2 + \frac{\partial^2}{\partial \bar{z}^{*2}} \right) \bar{C}, \tag{10}$$

where

$$\ell^2 = \frac{1}{\bar{r}} \frac{\partial}{\partial \bar{r}} \left(\bar{r} \frac{\partial}{\partial \bar{r}} \right). \tag{11}$$

According to Gill and Sankarasubramanian [28], the initial condition of convective diffusion coefficient is given by

$$\bar{C}(\bar{r},\bar{z},0) = \begin{cases} C_0 & \text{if } |\bar{z}| \le \dfrac{\bar{z}_s}{2}, \\ 0 & \text{if } |\bar{z}| > \dfrac{\bar{z}_s}{2}, \end{cases} \qquad (12)$$

where C_0 is the concentration referenced and $\bar{z}_s$ is the solute's length. The boundary condition following Gill and Sankarasubramanian [28] is

$$\bar{C}(\bar{r},\infty,\bar{t}) = 0, \qquad (13)$$

for symmetry at the central circular pipe $\bar{r} = 0$, the boundary condition is

$$\frac{\partial \bar{C}}{\partial \bar{r}}(0,\bar{z},\bar{t}) = 0 \qquad (14)$$

and for the solute concentration gradient at the wall $\bar{r} = \bar{R}(\bar{z})$, the boundary condition is given by

$$\frac{\partial \bar{C}}{\partial \bar{r}}(\bar{R}(\bar{z}),\bar{z},\bar{t}) = 0. \qquad (15)$$

2.3 Non-dimensional Variables

The non-dimensional variables are as follows

$$r = \frac{\bar{r}}{R_0}, \ \tau = \frac{\bar{\tau} R_0}{\bar{\mu} u_0}, \ p = \frac{\bar{p}\bar{\mu} u_0}{R_0}, \ z = \frac{\bar{z}}{R_0}, \ u = \frac{\bar{u}}{u_0}, \ \tau_y = \frac{\bar{\tau}_y R_0}{\bar{\mu} u_0}, \ u_s = \frac{\bar{u}_s}{u_0}, \ R(z) = \frac{\bar{R}(z)}{R_0},$$

$$E_z = \frac{\bar{E}_z}{\varepsilon}, \ r_p = \frac{\bar{r}_0}{R_0}, \ H = \frac{\bar{H}}{H_0}, C = \frac{\bar{C}}{C_0}, \ z^* = \frac{\bar{D}_m \bar{z}^*}{R_0^2 u_0}, \ z_s = \frac{\bar{D}_m \bar{z}_s}{R_0^2 u_0}, \ t = \frac{\bar{D}_m \bar{t}}{\bar{a}^2}, \qquad (16)$$

where u_0 is the fluid characteristic velocity. Here, r, τ, p, R_0, z/z^*, u, τ_y, u_s, $R(z)$, E_z, r_p, C, z_s, ε and t are radial coordinate, shear stress, pressure gradient, radius of artery in outer region, radial direction, velocity, yield stress, slip velocity, stenosed radius respectively in non-dimensional variables, electrical field in non-axial coordinate, radius of artery in plug flow region, solute concentration, solute length, electrical permittivity and time.

2.4 Method of Solution

The non-dimensional momentum equation obtained by substituting Eq. (16) into Eq. (1), it yields

$$\mu\left[\frac{1}{r}\frac{d}{dr}(r\tau)\right] - \frac{dp}{dz} + \sigma\rho_e \varepsilon E_z = 0. \qquad (17)$$

Integrate Eq. (17) with respect to r, it yields

$$\tau = \frac{r}{2\mu}\left[\frac{dp}{dz} - \sigma\rho_e\varepsilon E_z\right] + A_1, \tag{18}$$

where A_1 is a constant of integration. By substituting Eq. (16) into Eq. (2), the non-dimensional boundary condition of momentum equation is given as

$$\tau = \text{finite at } r = 0. \tag{19}$$

Substituting Eq. (19) into Eq. (18), it yields

$$\tau = \frac{r}{2\mu}\left[\frac{dp}{dz} - \sigma\rho_e\varepsilon E_z\right]. \tag{20}$$

Substituting $r = r_p$ and $\tau = \tau_y$ into Eq. (20) to form yield stress, τ_y, it yields

$$\tau_y = \frac{r_p}{2\mu}\left[\frac{dp}{dz} - \sigma\rho_e\varepsilon E_z\right]. \tag{21}$$

Substituting Eq. (16) into Eq. (3), the non-dimensional constitutive equation of Casson fluid is given by

$$-\frac{du}{dr} = \begin{cases} \frac{1}{\mu}\left(\sqrt{\tau} - \sqrt{\tau_y}\right)^2 & \text{if } \tau > \tau_y, \\ 0 & \text{if } \tau \le \tau_y. \end{cases} \tag{22}$$

Substituting Eq. (20) and (21) into Eq. (22), it yields

$$-\frac{du}{dr} = \frac{1}{\mu}\left[\frac{r}{2\mu}\left[\frac{dp}{dz} - \sigma\rho_e\varepsilon E_z\right] + \frac{r_p}{2\mu}\left[\frac{dp}{dz} - \sigma\rho_e\varepsilon E_z\right] - 2\sqrt{\frac{r}{2\mu}\left[\frac{dp}{dz} - \sigma\rho_e\varepsilon E_z\right]}\sqrt{\frac{r_p}{2\mu}\left[\frac{dp}{dz} - \sigma\rho_e\varepsilon E_z\right]}\right]. \tag{23}$$

Simplify Eq. (23), it becomes

$$-\frac{du}{dr} = \frac{1}{2\mu^2}\left[\frac{dp}{dz} - \sigma\rho_e\varepsilon E_z\right]\left[r + r_p - 2\sqrt{r}\sqrt{r_p}\right]. \tag{24}$$

Integrate Eq. (24) with respect to r, it becomes

$$-u = \frac{1}{2\mu^2}\left[\frac{dp}{dz} - \sigma\rho_e\varepsilon E_z\right]\left[\frac{r^2}{2} + rr_p - \frac{4r^{\frac{3}{2}}\sqrt{r_p}}{3}\right] + A_2, \tag{25}$$

where A_2 is a constant integration. Substituting Eq. (16) into Eq. (4), the non-dimensional of slip boundary condition of constitutive equation is given as

$$u = u_s \text{ at } r = R(z).$$ (26)

Substituting Eq. (26) into Eq. (25), the non-dimensional of the expression of velocity in the outer non-plug core is given by

$$u(r) = \frac{1}{4\mu^2}\left[\frac{dp}{dz} - \sigma\rho_e\varepsilon E_z\right]\left[R^2(z) - r^2 + 2r_p R(z) - 2rr_p - \frac{8\sqrt{r_p}R^{\frac{3}{2}}(z)}{3} + \frac{8\sqrt{r_p}r^{\frac{3}{2}}}{3}\right] + u_s,$$ (27)

where dp/dz is the non-dimensional of axial pressure gradient. By evaluating $r = r_p$ in the Eq. (27), the non-dimensional of velocity of fluid in the plug flow region is given as follows

$$u(r_p) = \frac{1}{4\mu^2}\left[\frac{dp}{dz} - \sigma\rho_e\varepsilon E_z\right]\left[R^2(z) - r_p^2 + 2r_p R(z) - 2r_p^2 - \frac{8\sqrt{r_p}R^{\frac{3}{2}}(z)}{3} + \frac{8r_p^2}{3}\right] + u_s.$$ (28)

The non-dimensional of mean velocity in Eq. (8) is given by

$$u_m = \int_0^{2\pi}\int_0^{R(z)}\frac{urdrd\theta}{rdrd\theta}$$ (29)

and has been solved using integral method. It forms

$$u_m = \frac{1}{8\mu^2}\left[\frac{dp}{dz} - \sigma\rho_e\varepsilon E_z\right]\left[R^2(z) + \frac{4}{3}r_p R(z) - \frac{16}{7}\sqrt{r_p}R^{\frac{3}{2}}(z) - \frac{1}{21}\frac{r_p^4}{R^2(z)} + u_s\right].$$ (30)

By applying Eq. (10) into Eq. (16), it is simplified as follows

$$\frac{\partial C}{\partial t} + u\frac{\partial C}{\partial z^*} = \left(\ell^2 + \frac{1}{Pe^2}\frac{\partial^2}{\partial z^{*2}}\right)C,$$ (31)

where

$$Pe = \frac{R_0 u_0}{D_m}.$$ (32)

Here, Pe is the Peclet number for the flow in a circular pipe which is given by Dash *et al.,* [30]. By using approach of Gill and Sankarasubramanian [28] and by assuming the solution of Eq. (31) as a derivative series expansion involving $\partial^i C_m/\partial z_1^i$ is shown as follows

$$C(r,z,t) = C_m(z_1,t) + \sum_{i=1}^{\infty} f_i(r,t) \frac{\partial^i C_m(z_1,t)}{\partial z_1^i}, \tag{33}$$

where C_m is the mean concentration of the solute over a cross-sectional area of the geometry, $f_i(r,t)$ is the dispersion function associated with $\partial^i C_m / \partial z_1^i$. By applying Eq. (12)-(15) into Eq. (16), the non-dimensional of initial and boundary conditions of convective-diffusion equation are obtained as

$$C(r,z,0) = \begin{cases} 1 \text{ if } |z| \le \dfrac{z_s}{2}, \\ 0 \text{ if } |z| > \dfrac{z_s}{2}, \end{cases} \tag{34}$$

$$C(r,\infty,t) = 0, \tag{35}$$

$$\frac{\partial C}{\partial r}(0,z,t) = 0, \tag{36}$$

$$\frac{\partial C}{\partial r}(R(z),z,t) = 0. \tag{37}$$

Using the initial condition Eq. (34) into Eq. (39), it yields $f_0(r,0) = 1$. Multiplying the solution in Eq. (39) with r and integrating it from 0 to $R(z)$ with the respect to r, it yields

$$C_m(z_1,t) = 2 \int_0^{R(z)} C(r,z_1,t)r \, dr. \tag{38}$$

According to Gill and Sankarasubramanian [28], the GDM is a derivative series expansion which given as

$$\frac{\partial C_m}{\partial t}(z_1,t) = \sum_{i=1}^{\infty} K_i(t) \frac{\partial^i C_m}{\partial z_1^i}(z_1,t), \tag{39}$$

where $K_i(t)$ is the transport coefficient given by

$$K_i(t) = \frac{\delta_{i2}}{\partial t} + 2 \frac{\partial f_i}{\partial r}(1,t) - 2 \int_0^{R(z)} f_{i-1}(r,t) u(r)r \, dr, \quad i = 1,2,3,\ldots, \tag{40}$$

with the Kronecker delta, $K_1(t)$ and $K_2(t)$ are the longitudinal convection coefficient and longitudinal diffusion coefficient from the Eq. (40). In terms of simple diffusion, the coefficient $K_2(t)$ reflects the entire dispersion process. It is known as the effective axial diffusivity. δ_{ij} is given by

$$\delta_{ij} = \begin{cases} 0 \text{ if } i \neq j, \\ 1 \text{ if } i = j. \end{cases} \tag{41}$$

The dispersion function of $f_1(r,t)$ plays an important role in calculating the mean concentration, $C_m(z_1,t)$. The dispersion function is given as follows

$$f_1(r,t) = f_{1s}(r) + f_{1t}(r,t), \tag{42}$$

where $f_{1s}(r)$ is the steady state dispersion function and $f_{1t}(r,t)$ is the dispersion function in the unsteady state that characterises the solute's time-dependent dispersion. The dispersion function at steady state is given by

$$\frac{1}{r}\frac{\partial}{\partial r}\left(r\frac{\partial f_{1s_-}}{\partial r}\right) - \left(u(r_p) - u_m\right) = 0 \text{ if } 0 \leq r \leq r_p \tag{43}$$

and the dispersion function in outer region is given as follows

$$\frac{1}{r}\frac{\partial}{\partial r}\left(r\frac{\partial f_{1s_-}}{\partial r}\right) - \left(u(r) - u_m\right) = 0 \text{ if } r_p \leq r \leq R(z). \tag{44}$$

Eq. (43) and Eq. (44) are solved using Eq. (44) to get f_{1s_-} and f_{1s_+}

$$\frac{df_{1s}}{dt}(0) = 0 \tag{45}$$

$$\frac{df_{1s}}{dr}R(z) = 0. \tag{46}$$

The steady dispersion function in the plug flow region, f_{1s_-} and outer flow region, f_{1s_+}. Thus, it yields

$$f_{1s_-} = CI - \frac{Ar^2 r_p^2}{48} + \frac{Ar^2 r_p^4}{672 R^2(z)} + \frac{1}{12}Ar^2 r_p R(z) - \frac{2}{21}Ar^2\sqrt{r_p}R^{\frac{3}{2}}(z) + \frac{1}{32}Ar^2 R^2(z) \tag{47}$$

$$f_{1s_+} = CI - \frac{Ar^4}{64} + \frac{8}{147}Ar^{\frac{7}{2}}\sqrt{r_p} - \frac{1}{18}Ar^3 r_p - \frac{115Ar_p^4}{28224} + \frac{Ar^2 r_p^4}{672 R^2(z)} + \frac{1}{12}Ar^2 r_p R(z) - \frac{2}{21}Ar^2\sqrt{r_p}R^{\frac{3}{2}}(z)$$
$$+ \frac{1}{32}Ar^2 R^2(z) - \frac{1}{336}Ar_p^4 \log(r) + \frac{1}{336}Ar_p^4 \log(r_p), \tag{48}$$

where $A = \frac{1}{8\mu^2}\left[\frac{dp}{dz} - \sigma\rho_e \varepsilon E_z\right]$ and

$$CI = A \left(\frac{13r_p^4}{7056} + \frac{r_p^6}{5280R^2(z)} - \frac{7r_pR^3(z)}{360} + \frac{15\sqrt{r_p}R^{\frac{7}{2}}(z)}{539} - \frac{R^4(z)}{96} - \frac{r_p^4}{336}\log(r_p) + \frac{1}{336}r_p^4\log(R(z)) \right). \qquad (49)$$

The general solution of $f_{1t}(r,t)$ is given as

$$f_{1t}(r,t) = \sum_{m=1}^{\infty} A_m e^{-\lambda_m^2 t} J_0(\lambda_m r), \qquad (50)$$

where

$$A_m = -\frac{2}{J_0^2(\lambda_m)} \int_0^{R(z)} J_0(\lambda_m r) f_{1s}(r) r dr. \qquad (51)$$

The mean concentration is obtained using Inverse Fourier Transform (IFT) [39]. It is given as follows

$$C_m(z_1,t) = \frac{1}{2}\left[erf\left(\frac{\frac{z_s}{2-z_1}}{2\sqrt{\xi}} \right) + erf\left(\frac{\frac{z_s}{2+z_1}}{2\sqrt{\xi}} \right) \right]. \qquad (52)$$

The manuscript does not include the full mathematical formulas for the mean concentration due to the intricacy of the calculations, which required the use of *Mathematica* to solve. This is due to the expressions are very large.

3. Results and Discussion

The current work investigated the effects of a Casson fluid model and an electric field on solute dispersion in blood passing through an artery, which is a circular, straight conduit. The GDM has been used in the research to achieve this. Samples of blood are extracted using the Casson fluid model. Including the electric field in the study helps to provide a more thorough understanding of the advances in medical treatments. The velocity, u, steady dispersion function, f_{1s}, unsteady dispersion function, f_{1t}, dispersion function, f_1 and mean concentration, C_m have been analysed. A graphic comparison of Newtonian and non-Newtonian systems has been presented. The behaviour of the fluid influencing the solute dispersion process has also been studied in more detail in the plug core area, r_p.

3.1 Velocity in Blood Flow

The effect of electric field, E_z and plug core region, r_p are computed graphically in this section. After the momentum equation is solved and the yield stress is established, the velocity results are produced and explained by varying various factors within the flow analytic expression.

The Casson fluid's velocity in relation to the electric field is illustrated in Figure 2, and the result has been validated by Dash *et al.,* [30]. The result for Casson fluid without the effect of an electric field shows a good result with the Casson fluid's velocity in the previous study [30]. It is depicted that the velocity in relation to the electric field in the present study is in good agreement with the velocity shown in Dash *et al.,* [30]. In the present study, when the electric field and height of stenosis is absence $\left(E_z = 0, \ a = 0\right)$, the density of electric field, ρ_e and radius of stenosed, $R(z)$ are $\rho_e = 1$ and $R(z) = 1$.
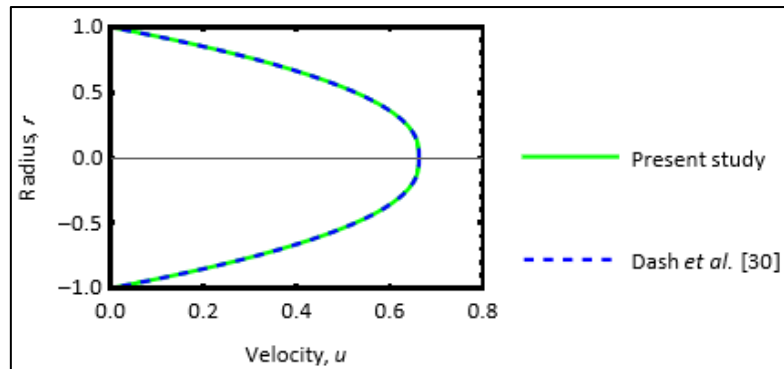
Fig. 2. Validation of present velocity with Dash *et al.,* [30]

Figure 3 illustrates the differencing of velocity, u for varied values of electric field, E_z in the blood flow with $a = 0.02$, $b = 2.5$, $z = 0.5$, $u_s = 0$, $\tau_y = 0.1$, $dp/dz = 2$, $\rho_e = 1$ and $\varepsilon = 1$ with varying electric field of $E_z = 0$, 0.2, 0.4, 0.6, 0.8. The electric field affects the blood velocity, and as the electric field increases, the velocity tends to increase. Blood flow is accelerated when an electrical field is applied perpendicular to its direction, which causes a discernible shift in the axial velocity distribution. The circulatory function is impacted by the rate of blood circulation and the size of blood vessels. Additionally, electrical stimulation can induce changes in physiology by initiating sympathetic tone through the contraction of muscles. Electrical stimulation has been found to augment venous return by increasing venous and muscle tension through sympathetic tone. This effect is advantageous in reducing the likelihood of pulmonary embolism and the occurrence of cardiac vein thrombus, as demonstrated by Jin *et al.,* [19]. Then, it is anticipated that as the electrical field increased, the axial velocity increased.

Figure 4 illustrates the differencing of velocity, u for varied values of plug core region, r_p in the blood flow with $a = 0.02$, $b = 2.5$, $.z = 0.5$, $u_s = 0$, $E_z = 1$, $dp/dz = 2$, $\rho_e = 1$ and $\varepsilon = 1$ with varying plug core region of $r_p = 0$, 0.02, 0.04, 0.06, 0.08. It can be noted that the plug flow region is skewed slightly towards the inner wall of the annulus. The plug core region is almost the entire annulus region, with the velocity in the plug core region being almost zero. The occurrence of stenosis hinders the circulation of blood in the constricted arteries, leading to alterations in yield stress. A rise in the frequency of the pulse results in a significant augmentation of the velocity of plug flow. According to Nagarani and Sarojamma [40], when the yield stress is inclined, there is a substantial diminution in the magnitude of velocity, leading to a large flow of the plug. Thus, the plug core region is inclined with the decreased velocity.
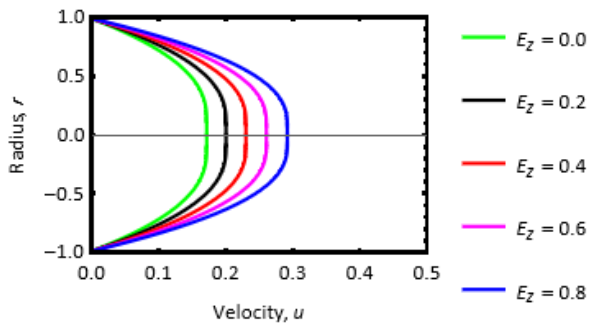
Fig. 3. Variation of velocity, u for varied values of electric field, E_z in the blood flow with $a = 0.02$, $b = 2.5, .\, z = 0.5$, $u_s = 0$, $\tau_y = 0.1$, $dp/dz = 2$, $\rho_e = 1$ and $\varepsilon = 1$
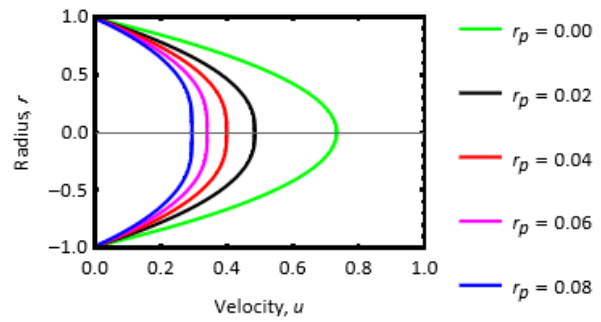
Fig. 4. Variation of velocity, u for varied values of plug core region, r_p in the blood flow with $a = 0.02$, $b = 2.5, .\, z = 0.5$, $u_s = 0$, $E_z = 1$, $dp/dz = 2$, $\rho_e = 1$ and $\varepsilon = 1$

3.2 Steady Dispersion Function

The dispersion function throughout the steady flow of Casson fluid through the blood vessel is investigated in this study. The dispersion function depends on the impact of an electric field on blood circulation through the artery. Gill and Sankarasubramanian [29] proposed the GDM in order to determine the transport coefficient.

The steady dispersion of Casson fluid with the effect of an electric field is illustrated in Figure 5, and the result has been validated by Dash *et al.,* [30]. Without the effect of an electric field, the result of Casson fluid's steady dispersion shows a good result in the present study [30]. It is depicted that the steady dispersion in relation to the electric field in the present study is in good agreement with the steady dispersion shown in Dash *et al.,* [30]. In the present study, when the electric field and height of stenosis is absence $\left(E_z = 0, \ a = 0 \right)$, the density of electric field, ρ_e and radius of stenosed, $R(z)$ are $\rho_e = 1$ and $R(z) = 1$.
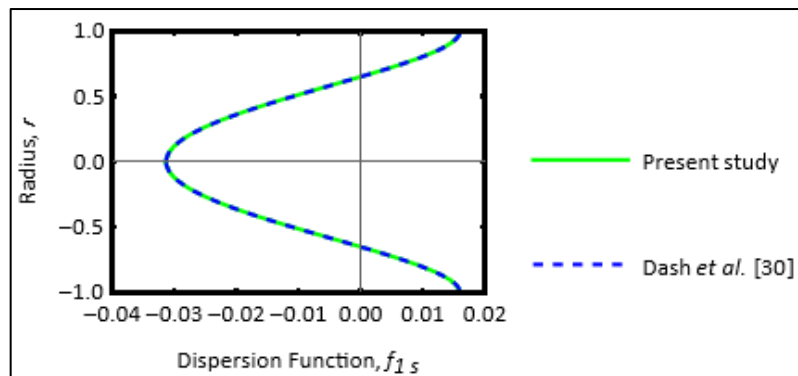
Fig. 5. Validation of present steady dispersion with Dash *et al.,* [30]

Figure 6 illustrates the differencing of steady dispersion function, f_{1s} for varied values of electric field, E_z in the blood flow with $a = 0.0001$, $dp/dz = 4$, $b = 0$, $z = 0.05$, $\tau_y = 0.1$, $\rho_e = 1$ and $\varepsilon = 1$ with varying electric field of $E_z = 0$, 0.2, 0.4, 0.6, 0.8. In this instance, the electric field impacts the dispersion function, causing the dispersion function to decrease. Physiological changes caused by electrical stimulation include an increase in blood flow and an effect on the peripheral circulation.

Electrical in vascular stenosis leads dispersion function to progressively grow. Due to the fact that the solute can migrate to the artery wall more quickly and effectively, it is crucial to increase the dispersion in the middle and decrease it close to the wall for better medicine outcomes.

Figure 7 illustrates the differencing of steady dispersion function, f_{1s} for varied values of plug core region, r_p in the blood flow with $a = 0.0001$, $dp/dz = 4$, $b = 0$, $z = 0.05$, $E_z = 1$, $\rho_e = 1$ and $\varepsilon = 1$ with varying plug core region of $r_p = 0.02$, 0.04, 0.06, 0.08, 0.1. From the figure, it shows that at the centre of the artery, the steady dispersion function of the solute increases as the plug core region increases, and the reverse behaviour occurs at the inner wall of the artery. The Casson fluid is classified as a non-Newtonian fluid due to its characteristic of exhibiting yield stress. This unique property renders it particularly suitable for applications involving restricted arterial conduits. The decline in the flow rate of the Casson fluid can be attributed to the increased fluid viscosity and the corresponding fall in the dispersion function value. The irregular and improper expansion of arterial walls can be attributed to stenosis or atherosclerosis, which occurs due to the excessive build-up of cholesterol and fat and aberrant tissue proliferation. According to Jaafar *et al.,* [41], the effective axial diffusion exhibits a gradual and consistent reduction as the plug core region increases.
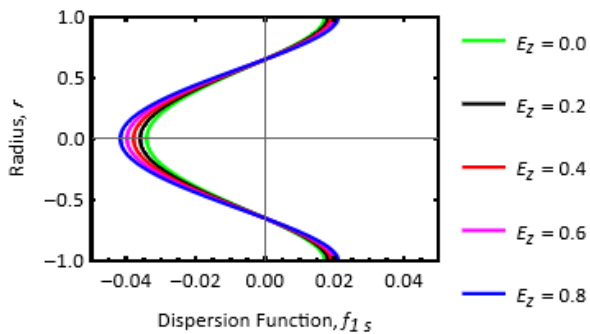
Fig. 6. Variation of steady dispersion function, f_{1s} for varied values of electric field, E_z in the blood flow with $a = 0.0001$, $dp/dz = 4$, $b = 0$, $z = 0.05$, $\tau_y = 0.1$, $\rho_e = 1$ and $\varepsilon = 1$
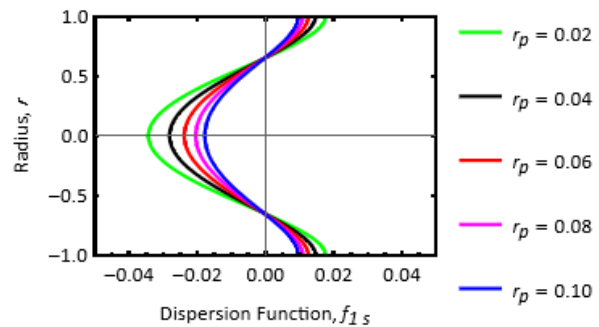
Fig. 7. Variation of steady dispersion function, f_{1s} for varied values of plug core region, r_p in the blood flow with $a = 0.0001$, $dp/dz = 4$, $b = 0$, $z = 0.05$, $E_z = 1$, $\rho_e = 1$ and $\varepsilon = 1$

3.3 Unsteady Dispersion Function

The dispersion phase throughout the unsteady flow of Casson fluid through an artery and velocity are investigated in this study. Gill and Sankarasubramanian [29] proposed the GDM in order to determine the transport coefficient. The dispersion function depends on the electric field.

Figure 8 illustrates the differencing of unsteady dispersion function, f_{1t} for varied values of electric field, E_z in the blood circulation with $a = 0.0001$, $dp/dz = 4$, $b = 0$, $z = 0.05$, $\tau_y = 0.01$, $\rho_e = 1$ and $\varepsilon = 1$ with varying electric field of $E_z = 0.1$, 0.5, 1, 1.5, 2. The increasing of time causes an increase in unsteady dispersion function. When time is at zero, the unsteady dispersion function shows the maximum results. Meanwhile, as time increased, the unsteady dispersion function increased near zero. Jaafar *et al.,* [35] have observed that the distribution of solutes in blood flow is influenced by two processes: red blood cell bending and migration to the core. This observation aligns with the findings of Patel and Sirs [42].

Figure 9 illustrates the differencing of unsteady dispersion function, f_{1t} for varied values of plug core region, r_p in the blood circulation with $a = 0.0001$, $dp/dz = 4$, $b = 0$, $z = 0.05$, $E_z = 1$, $\rho_e = 1$ and $\varepsilon = 1$ with varying plug core region of $r_p = 0.01$, 0.02, 0.03, 0.04, 0.05. As the plug core region increases, the unsteady dispersion function decreases. Non-Newtonian Casson fluid with yield stress is appropriate for narrow arteries. Since Casson fluid viscosity increased and dispersion function decreased, flow rate decreased. Simplified transport of solutes, like oxygen mixing with haemoglobin to generate oxyhaemoglobin, can complicate diffusion studies. Due to cell congestion, the plug flow has all the oxygen, and the boundary has limited oxygen [43]. The presence of many materials, particularly red blood cells, in the plasma results in blood being a concentrated suspension. As a result, red blood cell agglomeration and deformation may affect the lateral combining of any solute added to the bloodstream, which in turn can affect the rate of axial dispersion. According to Nagarani *et al.*, [43], the dispersion coefficients drop with the increased plug core region.
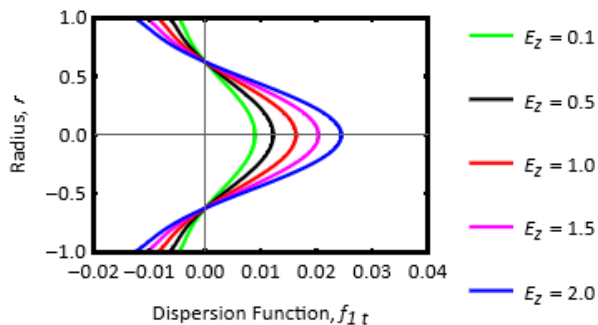
Fig. 8. Variation of unsteady dispersion function, f_{1t} for varied values of electric field, E_z in the blood flow with $a = 0.0001$, $dp/dz = 4$, $b = 0$, $z = 0.05$, $\tau_y = 0.01$, $\rho_e = 1$ and $\varepsilon = 1$
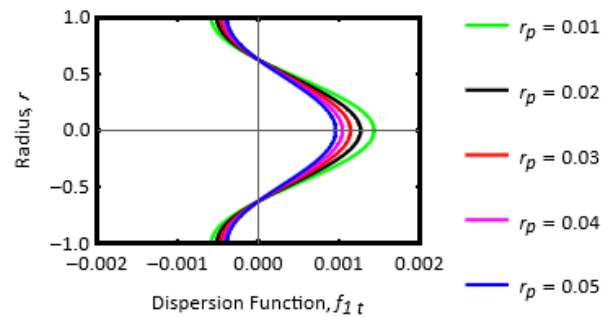
Fig. 9. Variation of unsteady dispersion function, f_{1t} for varied values of plug core region, r_p in the blood flow with $a = 0.0001$, $dp/dz = 4$, $b = 0$, $z = 0.05$, $E_z = 1$, $\rho_e = 1$ and $\varepsilon = 1$

3.4 Dispersion Function

Figure 10 illustrates the differencing of dispersion function, f_1 for varied values of electric field, E_z in the blood flow with $a = 0.0001$, $dp/dz = 4$, $b = 0$, $z = 0.05$, $\tau_y = 0.01$, $\rho_e = 1$ and $\varepsilon = 1$ with varying electric field of $E_z = 0$, 0.2, 0.4, 0.6, 0.8. The increasing value of the electric field tends to decrease the dispersion function. A graded membrane depolarization caused by electrical fields with biological characteristics depends on factors that are important for clinical practice (blood pressure and pulse rate) [17]. Therefore, as the electric field increased, the dispersion function declined.

Figure 11 illustrates the differencing of dispersion function, f_1 for varied values of plug core region, r_p in the blood flow with $a = 0.0001$, $dp/dz = 4$, $b = 0$, $z = 0.05$, $E_z = 1$, $\rho_e = 1$ and $\varepsilon = 1$ with varying plug core region of $r_p = 0.01$, 0.02, 0.03, 0.04, 0.05. The decrease in the dispersion function is observed with an inclination in the plug core region. Remarkably, the dispersion function reaches its greatest value when the plug core region is zero. The extent of solute dispersion is contingent upon the core radius of the plug, whereby an inclined core region of the plug leads to a corresponding inclined solute dispersion. The dispersion function exhibits its highest magnitude when the plug core

radius is zero, indicating that solute dispersion is maximized when there is no plug core present in the flow stream.
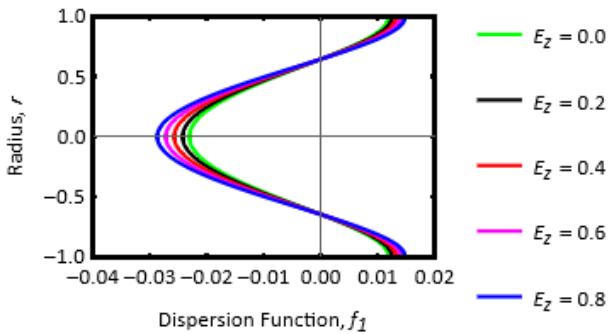
Fig. 10. Variation of dispersion function, f_1 for varied values of electric field, E_z in the blood flow with $a = 0.0001$, $dp/dz = 4$, $b = 0$, $z = 0.05$, $\tau_y = 0.01$, $\rho_e = 1$ and $\varepsilon = 1$
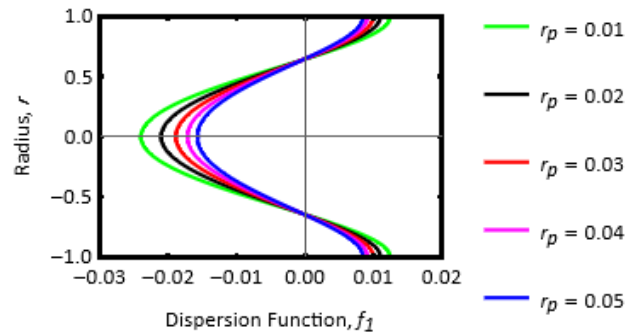
Fig. 11. Variation of dispersion function, f_1 for varied values of plug core region, r_p in the blood flow with $a = 0.0001$, $dp/dz = 4$, $b = 0$, $z = 0.05$, $E_z = 1$, $\rho_e = 1$ and $\varepsilon = 1$

3.5 Mean Concentration

The results of the mean concentration are useful to help the physiologist predict the correct dose needed for effectiveness. The mean concentration of Casson fluid is seen to increase when the drug reaches the bloodstream faster than it is extracted from the body. When a drug is extracted from the body, the average dose decreases continuously because the drug is removed from the body faster than it reaches the body.

Figure 12 illustrates the differencing of mean concentration, C_m for varied values of electric field, E_z in the blood circulation with $a = 0.0001$, $dp/dz = 10$, $b = 0$, $z = 0.05$, $\tau_y = 0.01$, $\rho_e = 1$ and $\varepsilon = 1$ with varying electric field of $E_z = 0$, 0.2, 0.4, 0.6, 0.8. The mean concentration increases with an increase in the electric field. As the solute concentration increased, the heart pumped blood at a high rate. With a higher mean concentration of solute at the highest-pressure gradient, solute dispersion, such as medication, reaches its maximum efficacy. Thus, the mean concentration increased when the effect of the electric field increased.

Figure 13 illustrates the differencing of mean concentration, C_m for varied values of plug core region, r_p in the blood flow with $a = 0.0001$, $dp/dz = 10$, $b = 0$, $z = 0.05$, $E_z = 1$, $\rho_e = 1$ and $\varepsilon = 1$ with varying plug core region of $r_p = 0.01$, 0.02, 0.03, 0.04, 0.05. The increase in the plug core region tends to decrease the mean concentration. The maximum mean concentration is the effective dose for the therapeutic concentration, and the therapeutic benefits as well as side effects of the drug can be expected by knowing the maximum concentration. In small-diameter arteries in round pipes, the average concentration of solute is higher. Therefore, as the plug core region increased, the mean concentration decreased.
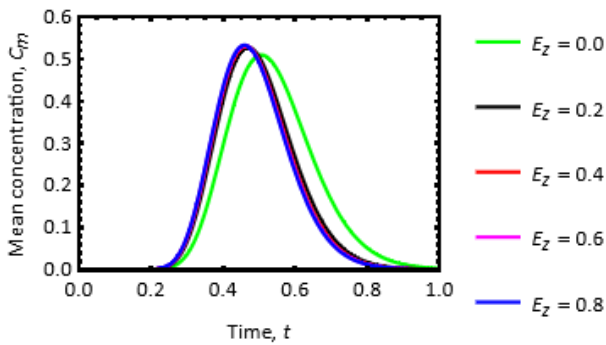
Fig. 12. Variation of mean concentration, C_m for varied values of electric field, E_z in the blood flow with $a = 0.0001$, $dp/dz = 10$, $b = 0$, $z = 0.05$, $\tau_y = 0.01$, $\rho_e = 1$ and $\varepsilon = 1$
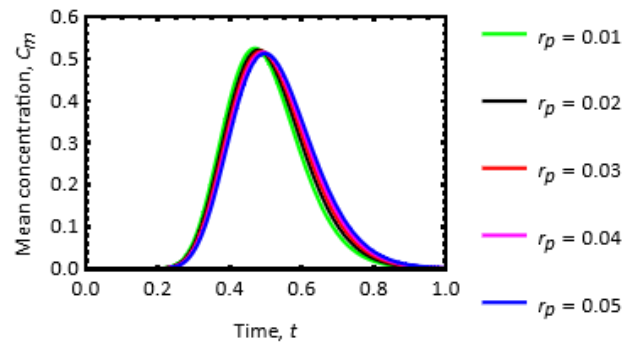
Fig. 13. Variation of mean concentration, C_m for varied values of plug core region, r_p in the blood flow with $a = 0.0001$, $dp/dz = 10$, $b = 0$, $z = 0.05$, $E_z = 1$, $\rho_e = 1$ and $\varepsilon = 1$

4. Conclusions

This study utilizes a novel methodology to analyse the effect of an electric field on solute dispersion within the Casson fluid model of blood circulation in arteries. This technique is grounded in the physiological realism of the cardiovascular system and aims to further understand the mixing process and drug distribution to tissues via arterial blood vessels. The effect of an electric field on velocity, stable and unsteady dispersion function, dispersion function, and mean concentration has been thoroughly examined. It has been determined that these characteristics significantly affect this quantity. The analytical solution of the dispersion function and mean concentration have been obtained by using GDM.

The results indicated an inclined electric field tends to be inclined in velocity, steady and unsteady dispersion function, and mean concentration. The reasoning is that the height of stenosis impacts the flow region of the blood flow. As the solute concentration increases, the heart pumps blood at a high rate. With a mean concentration of solute at the highest pressure gradient, solute dispersion reaches its maximum efficacy. Nonetheless, as the dispersion function decreases, the electric field increases. Not to mention, the dispersion function also decreases due to the lack of solute particles to diffuse efficiently across the artery axially. However, when the plug core region is considered in the problem, the solute dispersion behaves differently depending on the value of the plug core region. In an inclined plug core region, it decreases the velocity of flow, steady and unsteady dispersion functions, and mean concentration. This is due to the plug core region acting in the opposite direction of the solute, causing the impact of velocity, steady and unsteady dispersion function, and mean concentration to be reduced. Meanwhile, as the plug core region increases, the dispersion function increases. Similar to the electric field, the dispersion function also decreases due to the lack of solute particles to diffuse efficiently across the artery axially. Hence, in subsequent investigations, this study can be expanded to encompass two distinct models. It is important to acknowledge that the velocity and flow rate of the two-fluid blood flow model exhibit greater magnitudes compared to those of the single-fluid blood flow model.

Funding

Penerbit
Akademia Baru

References

1. Shah, Pallav Dhanendrakumar, Ashish Tiwari, and Satyendra Singh Chauhan. "Solute dispersion in micropolar-Newtonian fluid flowing through porous layered tubes with absorbing walls." *International Communications in Heat and Mass Transfer* 119 (2020): 104724. https://doi.org/10.1016/j.icheatmasstransfer.2020.104724

2. Chauhan, Satyendra Singh, and Ashish Tiwari. "Solute dispersion in non-Newtonian fluids flow through small blood vessels: A varying viscosity approach." *European Journal of Mechanics-B/Fluids* 94 (2022): 200-211. https://doi.org/10.1016/j.euromechflu.2022.02.009

3. *Functions of blood: transport around the body* (n.d.). Give blood.

4. Manshadi, Mohammad KD, Mahsa Saadat, Mehdi Mohammadi, Milad Shamsi, Morteza Dejam, Reza Kamali, and Amir Sanati-Nezhad. "Delivery of magnetic micro/nanoparticles and magnetic-based drug/cargo into arterial flow for targeted therapy." *Drug delivery* 25, no. 1 (2018): 1963-1973. https://doi.org/10.1080/10717544.2018.1497106

5. *What is atherosclerosis?* (2022, March 24). National Heart, Lung and Blood Institute. https://www.nhlbi.nih.gov/health/atherosclerosis

6. Bernstein, S. (2022, November 10). How Chemotherapy Works, *WebMD*.

7. Blair, GW Scott. "An equation for the flow of blood, plasma and serum through glass capillaries." *Nature* 183, no. 4661 (1959): 613-614. https://doi.org/10.1038/183613a0

8. Casson. (1959). Rheology of disperse systems, in Flow Equation for Pigment Oil Suspensions of the Printing Ink Type. *Rheology of Disperse Systems, C. C. Mill, Ed.*, 84–102, Pergamon Press, London, UK.

9. Merrill, E. W., A. M. Benis, E. R. Gilliland, T. K. Sherwood, and E. W. Salzman. "Pressure-flow relations of human blood in hollow fibers at low flow rates." *Journal of Applied Physiology* 20, no. 5 (1965): 954-967. https://doi.org/10.1152/jappl.1965.20.5.954

10. Felman, A. (2023, February 9). What to know about cardiovascular disease, *Medical News Today*.

11. *Side Effects of Cancer Treatment* (2023, May 15). Centers for Disease Control and Prevention.

12. Roy, Ashis Kumar, Apu Kumar Saha, and Sudip Debnath. "Hydrodynamic dispersion of solute under homogeneous and heterogeneous reactions." *Int. J. Heat Technol.* 37, no. 2 (2019): 387-397. https://doi.org/10.18280/ijht.370203

13. Debnath, S., Saha, A. K., Siddheshwar, P. G., & Roy, A. K. "On dispersion of a reactive solute in a pulsatile flow of a two-fluid model." *Journal of Applied Fluid Mechanics* 12, no. 3 (2019): 987-1000. https://doi.org/10.29252/jafm.12.03.29101

14. Debnath, S., A. K. Saha, P. G. Siddheshwar, and A. K. Roy. "Dispersion of reactive species in Casson fluid flow." *Indian Journal of Pure and Applied Mathematics* 51 (2020): 1451-1469. https://doi.org/10.1007/s13226-020-0476-7

15. Ali, Amjad, Zainab Bukhari, Muhammad Umar, Muhammad Ali Ismail, and Zaheer Abbas. "Cu and cu-swcnt nanoparticles' suspension in pulsatile casson fluid flow via darcy–forchheimer porous channel with compliant walls: a prospective model for blood flow in stenosed arteries." *International Journal of Molecular Sciences* 22, no. 12 (2021): 6494. https://doi.org/10.3390/ijms22126494

16. Singh, Shalini, and P. V. S. N. Murthy. "Unsteady solute dispersion in pulsatile Luo and Kuang blood flow (K-L Model) in a tube with wall reactive absorption." *Journal of Non-Newtonian Fluid Mechanics* 310 (2022): 104928. https://doi.org/10.1016/j.jnnfm.2022.104928

17. Trivedi, Darshan P., Kevin J. Hallock, and Peter R. Bergethon. "Electric fields caused by blood flow modulate vascular endothelial electrophysiology and nitric oxide production." *Bioelectromagnetics* 34, no. 1 (2013): 22-30. https://doi.org/10.1002/bem.21741

18. Shit, G. C., M. Roy, and A. Sinha. "Mathematical modelling of blood flow through a tapered overlapping stenosed artery with variable viscosity." *Applied Bionics and Biomechanics* 11, no. 4 (2014): 185-195. https://doi.org/10.1155/2014/698750

19. Jin, Hee-Kyung, Tae-Yeon Hwang, and Sung-Hyoun Cho. "Effect of electrical stimulation on blood flow velocity and vessel size." *Open Medicine* 12, no. 1 (2017): 5-11. https://doi.org/10.1515/med-2017-0002

20. Tripathi, Dharmendra, Ravinder Jhorar, Abhilesh Borode, and O. Anwar Bég. "Three-layered electro-osmosis modulated blood flow through a microchannel." *European Journal of Mechanics-B/Fluids* 72 (2018): 391-402. https://doi.org/10.1016/j.euromechflu.2018.03.016

21. Tripathi, Dharmendra, Jayavel Prakash, Abhishek K. Tiwari, and Rahmat Ellahi. "Thermal, microrotation, electromagnetic field and nanoparticle shape effects on Cu-CuO/blood flow in microvascular vessels." *Microvascular Research* 132 (2020): 104065. https://doi.org/10.1016/j.mvr.2020.104065

22. Ramasamy, Ponalagusamy, and D. Murugan. "Transport of a reactive solute in electro-osmotic pulsatile flow of non-newtonian fluid through a circular conduit." *Authorea Preprints* (2022). https://doi.org/10.22541/au.165389042.24480262/v1

23. Murugan, D., Ashis Kumar Roy, R. Ponalagusamy, and O. Anwar Bég. "Tracer dispersion due to pulsatile casson fluid flow in a circular tube with chemical reaction modulated by externally applied electromagnetic fields." *International Journal of Applied and Computational Mathematics* 8, no. 5 (2022): 221. https://doi.org/10.1007/s40819-022-01412-3

24. Ponalagusamy, R., and D. Murugan. "Transport of a reactive solute in electroosmotic pulsatile flow of non-Newtonian fluid through a circular conduit." *Chinese Journal of Physics* 81 (2023): 243-269. https://doi.org/10.1016/j.cjph.2022.11.002

25. Taylor, Geoffrey Ingram. "Dispersion of soluble matter in solvent flowing slowly through a tube." *Proceedings of the Royal Society of London. Series A. Mathematical and Physical Sciences* 219, no. 1137 (1953): 186-203. https://doi.org/10.1098/rspa.1953.0139

26. Aris, Rutherford. "On the dispersion of a solute in a fluid flowing through a tube." *Proceedings of the Royal Society of London. Series A. Mathematical and Physical Sciences* 235, no. 1200 (1956): 67-77. https://doi.org/10.1098/rspa.1956.0065

27. Gill, WN-Na5233. "A note on the solution of transient dispersion problems." *Proceedings of the Royal Society of London. Series A. Mathematical and Physical Sciences* 298, no. 1454 (1967): 335-339. https://doi.org/10.1098/rspa.1967.0107

28. Gill, W. N., and R. Sankarasubramanian. "Exact analysis of unsteady convective diffusion." *Proceedings of the Royal Society of London. A. Mathematical and Physical Sciences* 316, no. 1526 (1970): 341-350. https://doi.org/10.1098/rspa.1970.0083

29. Gill, W. N., and R. Sankarasubramanian. "Unsteady convective diffusion with interphase mass transfer." *Proceedings of the Royal Society of London. A. Mathematical and Physical Sciences* 333, no. 1592 (1973): 115-132. https://doi.org/10.1098/rspa.1973.0051

30. Dash, R. K., G. Jayaraman, and K. N. Mehta. "Shear augmented dispersion of a solute in a Casson fluid flowing in a conduit." *Annals of Biomedical Engineering* 28 (2000): 373-385. https://doi.org/10.1114/1.287

31. Rana, Jyotirmoy, and P. V. S. N. Murthy. "Solute dispersion in pulsatile Casson fluid flow in a tube with wall absorption." *Journal of Fluid Mechanics* 793 (2016): 877-914. https://doi.org/10.1017/jfm.2016.155

32. Rana, Jyotirmoy, and P. V. S. N. Murthy. "Unsteady solute dispersion in small blood vessels using a two-phase Casson model." *Proceedings of the Royal Society A: Mathematical, Physical and Engineering Sciences* 473, no. 2204 (2017): 20170427. https://doi.org/10.1098/rspa.2017.0427

33. Ratchagar, Nirmala P., and R. Vijayakumar. "Dispersion of a solute in a couple stress fluid with chemical reaction using generalized dispersion model." *Advances in Mathematics: Scientific Journal* 4, no. 9 (2020): 2233-2247. https://doi.org/10.37418/amsj.9.4.85

34. Guo, Jinlan, Weiquan Jiang, Guoqian Chen, Zhi Li, Njud S. Alharbi, and Muhammad Wakeel. "Solute dispersion in an open channel turbulent flow: Solution by a generalized model." *Journal of Hydrology* 604 (2022): 127239. https://doi.org/10.1016/j.jhydrol.2021.127239

35. Jaafar, Nurul Aini, Siti NurulAifa Mohd ZainulAbidin, Zuhaila Ismail, and Ahmad Qushairi Mohamad. "Mathematical analysis of unsteady solute dispersion with chemical reaction through a stenosed artery." *Journal of Advanced Research in Fluid Mechanics and Thermal Sciences* 86, no. 2 (2021): 56-73. https://doi.org/10.37934/arfmts.86.2.5673

36. Tiwari, Ashish, Pallav Dhanendrakumar Shah, and Satyendra Singh Chauhan. "Unsteady solute dispersion in two-fluid flowing through narrow tubes: A temperature-dependent viscosity approach." *International Journal of Thermal Sciences* 161 (2021): 106651. https://doi.org/10.1016/j.ijthermalsci.2020.106651

37. Tripathi, Dharmendra, Ashu Yadav, O. Anwar Bég, and Rakesh Kumar. "Study of microvascular non-Newtonian blood flow modulated by electroosmosis." *Microvascular Research* 117 (2018): 28-36. https://doi.org/10.1016/j.mvr.2018.01.001

38. Verma, Narendra Kumar, Shailesh Mishra, Shafi Ullah Siddiqui, and Ram Saran Gupta. "Effect of slip velocity on blood flow through a catheterized artery." *Applied mathematics* 2, no. 6 (2011): 764. https://doi.org/10.4236/am.2011.26102

39. Iida, Noriko. "Influence of plasma layer on steady blood flow in microvessels." *Japanese Journal of Applied Physics* 17, no. 1 (1978): 203. https://doi.org/10.1143/JJAP.17.203

40. Nagarani, P., and G. Sarojamma. "Effect of body acceleration on pulsatile flow of Casson fluid through a mild stenosed artery." *Korea-Australia Rheology Journal* 20, no. 4 (2008): 189-196.

41. Jaafar, Nurul Aini, Yazariah Mohd Yatim, and D. S. Sankar. "Mathematical analysis for unsteady dispersion of solute with chemical reaction in blood flow." In *AIP Conference Proceedings*, vol. 1750, no. 1. AIP Publishing, 2016. https://doi.org/10.1063/1.4954569

42. Patel, I. C., and J. A. Sirs. "Dispersion of solutes during blood flow through curved tubes." *Medical and Biological Engineering and Computing* 21 (1983): 113-118. https://doi.org/10.1007/BF02441524

43. Nagarani, P., G. Sarojamma, and G. Jayaraman. "Effect of boundary absorption in dispersion in Casson fluid flow in a tube." *Annals of Biomedical Engineering* 32 (2004): 706-719. https://doi.org/10.1023/B:ABME.0000030236.75826.8a

44. Dandu, Sridevi, Venkata Ramana Murthy Chitrapu, and Udaya Bhaskara Varma Nadimpalli. "Radiation Absorption and Diffusion Thermo Effects on Unsteady MHD Casson Fluid Flow Past a Moving Inclined Plate Embedded in Porous Medium in the Presence of Chemical Reaction and Thermal Radiation." *Journal of Advanced Research in Applied Sciences and Engineering Technology* 3 (2023): 92-107. https://doi.org/10.37934/araset.32.3.92107

45. Yahaya, Rusya Iryanti, Norihan Md Arifin, and Siti Suzilliana Putri Mohamed Isa. "Stability Analysis on Magnetohydrodynamic Flow of Casson Fluid over a Shrinking Sheet with Homogeneous-Heterogeneous Reactions." *Entropy* 20(9) (2018): 652. https://doi.org/10.3390/e20090652

46. Omar, Nur Fatihah Mod, Husna Izzati Osman, Ahmad Qushairi Mohamad, Rahimah Jusoh, and Zulkhibri Ismail. "Analytical Solution of Unsteady MHD Casson Fluid with Thermal Radiation and Chemical Reaction in Porous Medium." *Journal of Advanced Research in Applied Sciences and Engineering Technology* 2 (2023): 185-194. https://doi.org/10.37934/araset.29.2.185194

47. Azmi, Wan Faezah Wan, Ahmad Qushairi Mohamad, Yeou Jiann Lim, and Sharidan Shafie. "Slip Velocity Effect on Unsteady Free Convection Flow of Casson Fluid in a Vertical Cylinder." *CFD Letters* 5 (2023): 29-41. https ://doi.org/10.37934/cfdl.15.5.2941

48. Arifin, Nur Syamilah, Abdul Rahman Mohd Kasim, Syazwani Mohd Zokri, Siti Farah Haryatie, and Mohd Zuki Salleh. "Dusty Casson Fluid Flow containing Single-Wall Carbon Nanotubes with Aligned Magnetic Field Effect over a Stretching Sheet." *CFD Letters* 1 (2023): 17-25. https://doi.org/10.37934/cfdl.15.1.1725

49. Mohamed, Muhammad Khairul Anuar, Siti Hanani Mat Yasin, and Mohd Zuki Salleh. "Slip Effects on MHD Boundary Layer Flow over a Flat Plate in Casson Ferrofluid." *Journal of Advanced Research in Fluid Mechanics and Thermal Sciences* 1 (2021): 49-57. https://doi.org/10.37934/arfmts.88.1.4957